agronomy

MDPI

Article

Assessment of Alkali Tolerance and Transcriptome Profiling of In Vitro Potato Under $NaHCO_3$ Stress

Xia Zhang [1,*,†], Shuangshuang Zheng [1,†], Caicai Lin [1], Haiyan Wang [2], Han Zhang [2], Zhonghao Liu [2], Jingjie Xu [2], Qingshuai Chen [1], Ru Yu [1], Suhui Lv [1], Peiyan Guan [3] and Linshuang Hu [1,*]

[1] Institute of Biophysics, Dezhou University, Dezhou 253023, China; zssadu@163.com (S.Z.); lcc@dzu.edu.cn (C.L.); qingschen_dzu@dzu.edu.cn (Q.C.); yuru@dzu.edu.cn (R.Y.); lvsuhui@dzu.edu.cn (S.L.)
[2] Belgorod Institute of Food Sciences, Dezhou University, Dezhou 253023, China; 17862633778@163.com (H.W.); 15098579328@163.com (H.Z.); 15163545956@163.com (Z.L.); 15254801955@163.com (J.X.)
[3] College of Life Science, Dezhou University, Dezhou 253023, China; peiyanguan@dzu.edu.cn
* Correspondence: zhangxia@dzu.edu.cn (X.Z.); hulinshuang@dzu.edu.cn (L.H.)
† These authors contributed equally to this work.

Abstract

Potato (*Solanum tuberosum* L.) is an important staple crop globally, and its growth and productivity are severely constrained by alkali stress. However, this crop's alkali tolerance and the molecular mechanisms mediating its responses to alkali stress have not been fully elucidated. In this study, a concentration gradient method was employed, and we determined that a $NaHCO_3$ concentration of 10 mM is optimal for inducing alkali stress. Subsequently, the morphological and physiological traits of 17 potato accessions were examined and evaluated. A comprehensive assessment of alkali tolerance was conducted using multivariate analytical methods—including principal component, membership function, and cluster analyses—leading to the development of a linear regression model: $A = 0.790 - 0.124\ RL + 0.000276\ CAT$ (*RL* represents the root length and *CAT* represents catalase). Transcriptomic analysis of selected alkali-tolerant and alkali-sensitive accessions identified 1283 differentially expressed genes (DEGs) that responded to alkali stress. Gene Ontology (GO) and Kyoto Encyclopedia of Genes and Genomes (KEGG) enrichment analyses indicated that potato's response to alkali stress is linked to peroxidase activity, oxidoreductase activity, and the phenylpropanoid biosynthesis pathway. Through hierarchical cluster and weighted correlation network analysis (WGCNA), 92 candidate genes were identified. Twelve of these DEGs were further validated via qRT-PCR, confirming that their expression patterns were consistent with the transcriptomic data. These findings offer a new perspective for the screening of alkali-tolerant potato cultivars and provide a valuable resource for the functional characterization of alkali-tolerance genes and future breeding efforts.

Keywords: *Solanum tuberosum* L.; alkali stress; $NaHCO_3$; transcriptome; tolerance assessment; WGCNA

Academic Editor: Xingwang Liu

Received: 27 October 2026
Revised: 26 November 2026
Accepted: 26 November 2026
Published: 29 November 2026

Copyright: © 2026 by the authors. Licensee MDPI, Basel, Switzerland. This article is an open access article distributed under the terms and conditions of the Creative Commons Attribution (CC BY) license.

1. Introduction

Soil alkali stress severely affects the sustainable development of global agriculture. More than 1 billion hectares of land worldwide are affected by soil salinization, resulting

in significant declines in crop yield and quality [1,2]. Soil saline–alkali components are mainly composed of neutral (NaCl) and alkali components ($NaHCO_3$ and Na_2CO_3) [3]. Compared with neutral salt stress alone, alkali stress inflicts more complex and severe damage on plants. It leads to an elevated pH that directly damages roots, hinders nutrient and mineral uptake and utilization, and disrupts ion homeostasis, thereby causing greater harm to crops [1,4]. Therefore, screening alkali-tolerant germplasm resources is a prerequisite for alkali-tolerant crop breeding.

The potato (*Solanum tuberosum* L.) contributes significantly to food security and economic development due to its high yield, nutritional value and adaptability. Crops such as rice, maize, and wheat are sensitive to salt stress, which inhibits root nutrient uptake, reduces carbon fixation and photosynthesis, and ultimately leads to yield reduction [5–7]. Potato is generally considered to possess a certain degree of salt–alkali tolerance and is regarded as an ideal crop for the development and utilization of saline–alkali soils. When compared with the alkali tolerance evaluation systems of other crops, most studies are found to have limited evaluation indicators, inconsistent stress concentrations and identification stages, and a lack of uniformity in evaluation criteria [8–10]. Although recent studies have revealed the roles of the ABA (abscisic acid)-PP2C-SnRK2s pathway and regulatory factors in the response to alkali stress from the perspectives of hormone signaling and transcriptional regulation [11], the integration of mechanistic research with a comprehensive evaluation system remains limited. Therefore, integrating multi-index comprehensive evaluation with transcriptomic analysis to dissect the molecular mechanisms based on precise screening of genotypes with contrasting alkali tolerance is of great significance for refining the alkali-tolerance evaluation system and promoting genetic improvement of alkali tolerance in potato.

Numerous studies have described the physiological and molecular mechanisms underlying salt stress responses in potato [12–14], and many salt-responsive genes and pathways have been identified [15–17]. Research on the mechanisms underlying alkali-stress responses in potato has mainly focused on hormone signaling, transcriptional regulation, and metabolism [18–20]. For example, the transcription factor *StbZIP1* positively regulates potato tolerance, with overexpression lines exhibiting 33–50% higher chlorophyll content and 81–104% greater superoxide dismutase (SOD) and peroxidase (POD) activities under stress compared with controls [21]. Experimental evidence also indicates that miRNAs contribute to alkali stress tolerance in potato. For instance, miR4243-x and novel-m064-5p are believed to play a role in the alkali stress response [22]. Exogenous spermidine improves alkali tolerance by regulating key genes such as *StHK4*, *StbZIP27*, and *StERF106*, integrating cytokinin-ABA signaling, osmotic regulation, and reactive oxygen species (ROS) scavenging [23]. These findings offer valuable insights into the molecular network of potato alkali stress responses, yet the regulatory mechanisms governing alkali tolerance remain poorly characterized from a systematical perspective.

In recent years, high-throughput RNA sequencing (RNA-Seq) has emerged as a powerful approach to link physiological phenotypes to the underlying molecular alterations associated with plant stress responses. This technology enables the quantification of differentially expressed genes, as well as the identification of enriched biological processes and regulatory networks [24]. Comparative transcriptome analysis between alkali-tolerant and sensitive genotypes under alkali stress allows the screening of differentially expressed genes (DEGs) involved in alkali stress responses, which can be further enriched in key pathways such as ion transport and homeostasis, potential of hydrogen (pH) regulation, ROS scavenging, hormone signaling, and transcriptional regulation [25–27]. These candidate genes and pathways provide an important basis for elucidating the molecular mechanisms that underlie alkali tolerance in potato. However,

the specific transcriptional mechanisms conferring alkali tolerance remain unclear, and the core genetic determinants have yet to be elucidated.

For this purpose, potato plantlets with contrasting alkali tolerance were used as materials. Under simulated $NaHCO_3$ alkali stress, phenotypic, physiological and biochemical indices were comprehensively evaluated to screen potato genotypes with stable tolerance differences. High-throughput transcriptome sequencing was used to compare gene expression profiles between alkali-tolerant and sensitive materials at key stress stages. We screened DEGs under alkali stress and carried out functional enrichment analysis, with candidate genes subsequently validated by quantitative real-time PCR (qRT-PCR). Distinct from previous studies, our work integrated this time-series transcriptomic profiling with long-term phenotypic and physiological measurements at 21 d; we further constructed co-expression networks to link early transcriptional reprogramming with the final alkali-tolerance phenotypes. The aims were to preliminarily construct a multi-index evaluation system for alkali tolerance in potato, identify superior alkali-tolerant germplasms, mine core stress-responsive genes, and provide an initial understanding of the molecular mechanisms and pathways responsible for alkali tolerance. These findings offer a theoretical basis and genetic evidence for marker-assisted breeding and deeper investigation of alkali tolerance in potato.

2. Materials and Methods

2.1. Plant Materials and Sample Collection

The potato tissue culture seedlings used in this study were tetraploid accessions obtained from the National Engineering Research Center for Potatoes (Table S1). Five accessions (Z1076-1, Z494, Z1264-1, Z1266-1 and Z1268-1) were used to screen and determine the optimal $NaHCO_3$ concentration for alkali tolerance evaluation. Two genotypes, Z943 and Z965, were selected for RNA-Seq analysis. Samples designated for morphological observation and physiological parameter analysis were collected after 21 days of alkali treatment on solid medium and stored at −20 °C. For transcriptome profiling, root tissues were collected from plantlets cultured in liquid medium. Single-leaf stem segments (measuring 1 cm in length) from potato plantlets pre-cultured on MS solid medium for 21 days were pre-cultured in standard liquid MS medium (pH 5.8) for 1 d. The seedlings were transferred to liquid MS medium supplemented with 10 mM $NaHCO_3$ (pH 8.2). Samples were collected at 0 h (control, CK) and after 24 h of treatment. Root samples were immediately snap-frozen in liquid nitrogen after collection and then stored at −80 °C. Three biological replicates were included at each sampling timepoint. Morphological and physiological traits were assessed at the 21-day timepoint to capture late-stage phenotypic responses. In contrast, transcriptome samples were collected at acute timepoints (0, 6, 12 and 24 h) to capture early transcriptional events. These short-time-point transcriptional changes reflect the initial stress perception and downstream signaling cascades, which are presumed to underpin the morphological and physiological alterations observed at 21 days.

2.2. Alkali Stress Treatments and Measurement of Alkali-Tolerance Indices

The alkali treatment and plant growth conditions were based on those reported in previous studies [11,22,28]. Briefly, MS solid medium [29] was supplemented with 0 (pH 5.8), 5 (pH 8.2), 10 (pH 8.2), 15 (pH 8.2) and 20 (pH 8.2) mM $NaHCO_3$ before autoclaving. Single-leaf stem segments (measuring 1 cm in length) from potato plantlets pre-cultured on MS solid medium for 21 days were inoculated onto the above media. The control plantlets were grown on untreated MS medium (pH 5.8). Each treatment contained three biological replicates, with five explants per replicate. The plantlets were cultured in a

growth chamber (Panasonic, MLR-3523-PC, Osaka, Japan) at (25 ± 2) °C under a 16 h light/8 h dark photoperiod with light intensity of 2000–3000 lx. A single-factor completely randomized design was applied to evaluate the effects of $NaHCO_3$-induced alkali stress on potato plantlet growth. After three weeks of treatment, morphological traits including plant height (PH), root length (RL), fresh weight (FW) and stem diameter (SD) were measured. The effective growth rate and coefficient of variation (CV) of each trait were calculated.

Based on the gradient stress results, an optimal $NaHCO_3$ concentration was selected to treat seedlings of 17 tetraploid potato genotypes. After three weeks of alkali stress, the morphological traits and key physiological indices of the plants were measured, including superoxide dismutase (SOD), peroxidase (POD), and catalase (CAT) activities, as well as their malondialdehyde (MDA) and proline (PRO) contents. To eliminate inherent differences among germplasms, all indices were converted into alkali tolerance coefficients and standardized into membership function values. Combined with principal component analysis, comprehensive alkali tolerance scores were obtained for each genotype, and cluster analysis was performed to classify germplasm tolerance [30–33].

We used the determination methods described by Khadka [34] and Rahman [35], with slight modifications. Potato seedlings treated with the solid media containing the various concentrations of $NaHCO_3$ described above were carefully removed from the media, rinsed, and then photographed using a digital camera (ILCE-7M3, Sony, Tokyo, Japan). Plant height and root length were quantified using ImageJ (ImageJ 1.48v) [36]. Seedlings were deemed to have demonstrated effective growth when the regenerated bud length exceeded 1 cm, leaves appeared normal, and no rosette had formed; all other seedlings were considered to be ineffective. The effective growth rate (%) = (number of effectively grown seedlings/15) × 100% [28]. The total number of seedlings for each accession was 15. The activities of SOD, POD and CAT, as well as the MDA and proline content, were measured using commercial assay kits from Solarbio Science & Technology Co., Ltd., Beijing, China. The corresponding catalog numbers are BC0175, BC0095, BC0205, BC0025 and BC0295, respectively. All assays were performed according to the manufacturer's protocol**s** [37–41].

2.3. Comprehensive Assessment Method of Alkali Tolerance Using Membership Function and Principal Component Analysis (PCA)

Membership function values derived from all measured traits were calculated to assess alkali tolerance across potato accessions. PCA (principal component analysis) was utilized to assign weights to each composite index. The alkali-tolerance coefficient for each parameter is defined as the ratio of the value measured under alkali stress to the value measured under normal conditions. The comprehensive alkali-tolerance coefficient (A) was calculated using the following formulas:

$$F(X_j) = a_{1j}X_{1j} + a_{2j}X_{2j} + \ldots + a_{ij}X_{ij}\ (i = 1, 2, \ldots, n;\ j = 1, 2, \ldots, n)$$

$$U(X_j) = (X_j - X_{min})/(X_{max} - X_{min})\ (j = 1, 2, 3, \ldots, n)$$

$$W_j = P_j/\sum_{j-1}^{n} P_j$$

$$A = \sum_{j-1}^{n} (U(X_j)W_j)\ (j = 1, 2, 3, \ldots, n)$$

where $F(X_j)$ refers to the *jth* comprehensive index value, a_{ij} is the factor load corresponding to the eigenvalue of each individual indicator, and X_{ij} represents the standardized processing value of each index. $U(X_j)$ indicates the membership function value of the *jth* indicator, X_j is the alkali-tolerance coefficient of the *jth* indicator, while X_{min} and X_{max}

represent the minimum and maximum values of the *jth* indicator, respectively. W_j is the weight of the *jth* principal component, P_j is the variance contribution rate of the *jth* principal component, and n is the number of retained principal components [42].

2.4. RNA Sequencing and Analysis

Total RNA was extracted from the root tissues of potato plantlets using the RNA prep Pure Plant Plus Kit (TIANGEN, Beijing, China). All RNA isolates underwent quality validation; RNA integrity was primarily evaluated via the Agilent 2100 Bioanalyzer (Agilent Technologies, Inc., Santa Clara, CA, USA). Qualified RNA samples were subjected to transcriptome library preparation with the Hieff NGS® Ultima Dual-mode RNA Library Prep Kit (Premixed version) (Yeasen, Shanghai, China), in accordance with the manufacturer's protocols. First, based on the fact that most eukaryotic mRNA contains a polyA tail, polyA-tailed mRNA was enriched using Oligo(dT) magnetic beads. Subsequently, the first strand of cDNA was synthesized, and immediately after the reaction, the second strand of cDNA was synthesized, followed by end repair/A-tailing. Specific MGI® adapters were ligated to the ends of the products. After adapter ligation, PCR amplification was performed to obtain the cDNA library. These steps are typical in conventional library construction. For sequencing on the DNBSEQ-T7 platform by Smartgenomics Technology Institute (Tianjin, China), to obtain DNA nanoballs, the double-stranded products from the cDNA library must undergo denaturation and circularization, followed by digestion, to obtain single-stranded circular cDNA for the preparation of DNA nanoballs.

Raw sequencing data commonly contain low-quality reads and residual adapter sequences. In this study, Fastp (v0.23.4, a tool for quality control and preprocessing of high-throughput sequencing reads) was run using its default parameters to filter out invalid reads [43]. Clean reads were mapped to the potato doubled monoploid reference genome DM1-3 516R44 (assembly v6.1) [44], downloaded from SpudDB (https://spuddb.uga.edu/dm_v6_1_download.shtml) (accessed on 13 April 2026). High-quality clean reads were aligned to the reference genome using HISAT2 (v2.2.1, Hierarchical Indexing for Spliced Alignment of Transcripts) [45]. Transcripts were assembled with StringTie (v2.2.3, Johns Hopkins University, Baltimore, MD, USA; http://ccb.jhu.edu/software/stringtie/index.shtml) (accessed on 18 April 2026). [46], and transcript sets from all samples were merged. FeatureCounts (v2.0.3, Parkville, VIC, Australia), an efficient general-purpose program for assigning sequence reads to genomic features, was employed to quantify the number of reads mapped to each gene [47], and FPKM (Fragments Per Kilobase of the exon model per Million mapped fragments) values were subsequently calculated for each gene based on its length and the corresponding mapped read count.

2.5. Detection of Differentially Expressed Transcripts

Differential expression analysis was performed using the edgeR package (v3.22.5) [48]. Read counts were normalized by scaling factors before analysis. The Benjamini–Hochberg procedure was used to adjust p values and control the false discovery rate. Genes satisfying the thresholds $|\log2(\text{FoldChange})| > 1.0$ and adjusted p (padj) ≤ 0.05 were identified as significantly differentially expressed.

2.6. Functional Enrichment and Co-Expression Network Analysis of DEGs

GO (Gene Ontology) and KEGG (Kyoto Encyclopedia of Genes and Genomes) enrichment analysis of DEGs was implemented. Gene functional annotations were derived from the potato DM v6.1 reference genome. All annotated genes in DM v6.1 were

used to establish the background. Terms with an adjusted $p < 0.05$ were defined as significantly enriched.

Genes with similar expression patterns were clustered using clusterProfiler (v4.14.5, Guangzhou, China) [49]. Weighted gene co-expression network analysis (WGCNA, v1.47) in R was used to construct such networks based on the gene expression matrix. Modules strongly associated with alkali stress responses were screened, and hub genes from key modules were analyzed using the contrasts Z943_24 h vs. Z943_CK and Z965_24 h vs. Z965_CK to identify candidate alkali-responsive genes.

2.7. Quantitative Real-Time Polymerase Chain Reaction (qRT-PCR) Validation

According to the transcriptome results, twelve candidate genes were selected for qRT-PCR validation. The reverse transcription of mRNA was performed using FastKing gDNA Dispelling RT SuperMix (Tiangen Biotech, Beijing, China). The qRT-PCR assays were run on a LightCycler96 system (Roche Applied Science, Basel, Switzerland) employing ChamQ Universal SYBR qPCR Master Mix (Vazyme, Nanjing, China). Potato Actin was used as the internal reference to normalize expression. Relative expression of the target genes was computed using the $2^{-\Delta\Delta Ct}$ method [50]. Three biological replicates and three technical replicates were included for each assay. All primer sequences are listed in Table S2.

2.8. Statistical Analysis

Statistical analyses were performed in SPSS 25.0 (IBM, Armonk, NY, USA). All data are presented as mean ± standard deviation (SD). One-way analysis of variance (ANOVA) followed by Tukey's or Dunnett's test was used to detect significant differences (* $p < 0.05$; ** $p < 0.01$). Means with different letters indicate significant differences at $p < 0.05$. Figures were generated using Origin 2021 (OriginLab, Corporation, Northampton, MA, USA) and SPSS 25.0.

3. Results

3.1. Screening of Suitable Alkali Stress Concentrations and Descriptive Statistical Analysis of Potato Plantlets Under Alkali Stress

Under alkali stress, plant height (PH), root length (RL), fresh weight (FW), and stem diameter (SD) were measured in five potato germplasm accessions (Z1076-1, Z494, Z1264-1, Z1266-1, Z1268-1). Figure 1 shows representative seedling phenotypes of these potato accessions across a gradient of $NaHCO_3$ concentrations, and Figure 2A–D present the quantitative data for each growth index. As the $NaHCO_3$ concentration increased, different growth parameters exhibited distinct response patterns. Stem diameter displayed a unimodal trend: it increased slightly under low-to-moderate alkali stress but decreased when stress intensity rose further. In contrast, plant height, root length, and fresh weight declined continuously with increasing $NaHCO_3$ concentration (Figure 2A–D). Significant genotypic differences were observed for all measured traits at 10 mM $NaHCO_3$. When the $NaHCO_3$ concentration reached 15 mM and 20 mM, the growth of most accessions was severely inhibited, and plant height, root length and fresh weight dropped to very low levels.

We further evaluated the effective growth rate of the five potato accessions (Figure 2E). The effective growth rate remained at 100% under 0 mM and 5 mM $NaHCO_3$, indicating that low concentrations of $NaHCO_3$ barely affected seedling growth. At 10 mM $NaHCO_3$, the effective growth rate decreased to approximately 80%, and clear phenotypic differentiation among genotypes was still detectable. At 15 mM and 20 mM $NaHCO_3$, the

effective growth rate declined sharply to 20–40%, accompanied by severe growth retardation of seedlings.

Collectively, 10 mM $NaHCO_3$ produced distinguishable phenotypic differences among the five potato genotypes without causing lethal damage. Accordingly, this concentration was selected as the optimal treatment condition for subsequent alkali tolerance evaluation of potato seedlings under in vitro tissue-culture conditions.

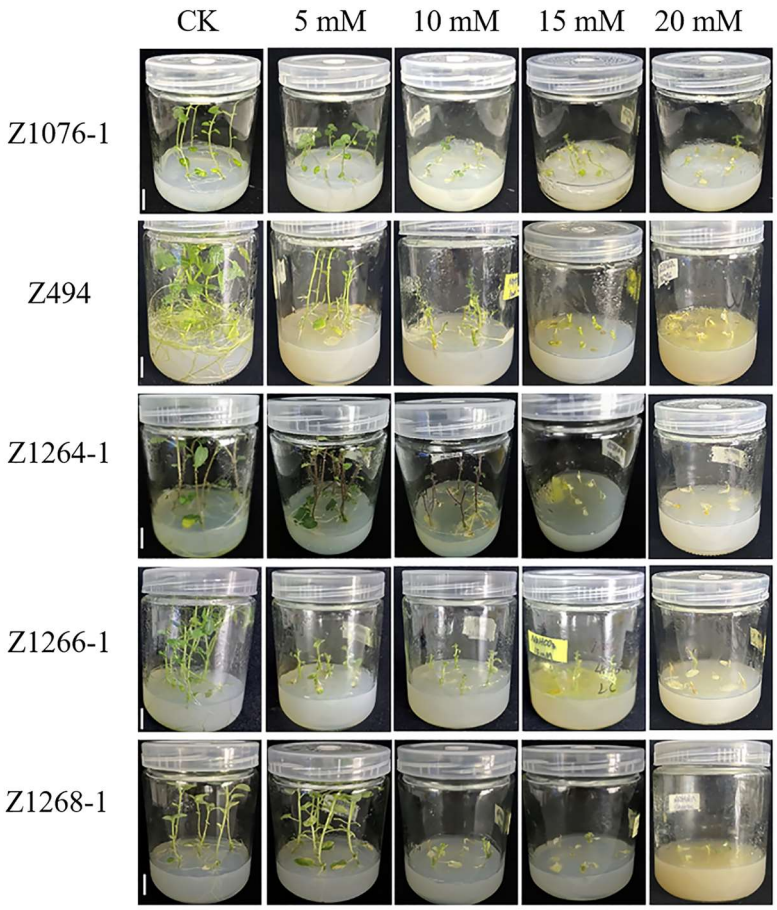
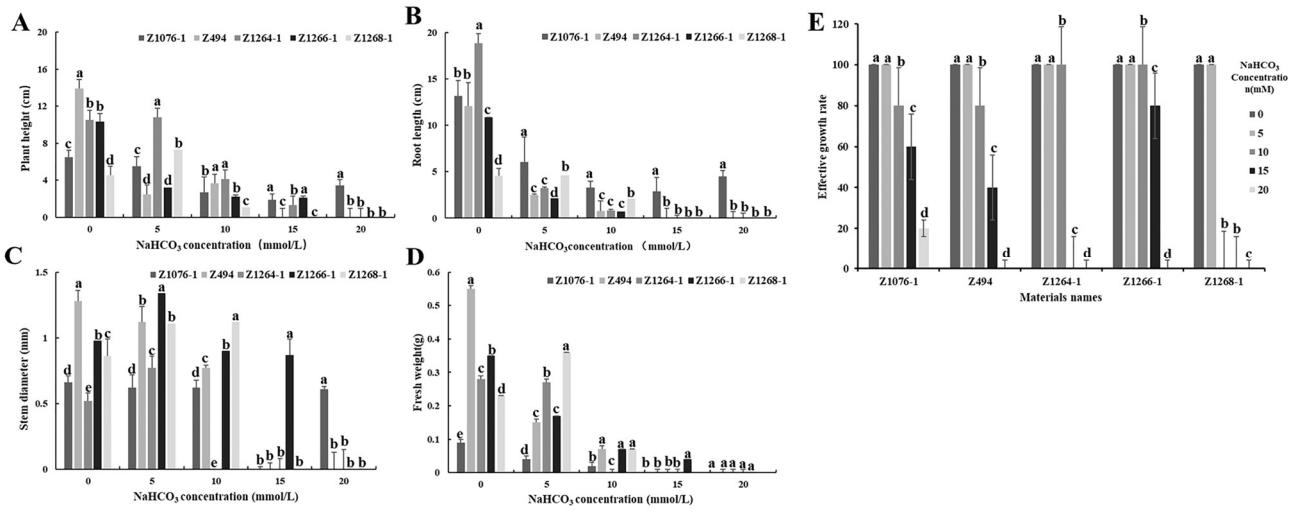


Figure 1. Phenotypic analysis of five potato accessions under different alkali concentrations. Five potato accessions grown on different media after 21 days. CK: MS solid medium; $NaHCO_3$ stress: MS solid media were supplemented with 5, 10, 15 and 20 mM $NaHCO_3$. Bar = 2 cm.



https://doi.org/10.3390/agronomy16232419

Figure 2. Phenotypic statistical analysis of five potato accessions under different alkali concentrations. (**A**): Statistical analysis of plant height; (**B**): Statistical analysis of root length; (**C**): Statistical analysis of stem diameter concentration treatments; (**D**): Statistical analysis of fresh weight; (**E**): Statistical analysis of effective growth rate. Different lowercase letters indicate significant differences at $p < 0.05$.

The morphological and physiological parameters of 17 potato accessions were quantified and statistically analyzed after 21 days of 10 mM $NaHCO_3$ exposure (Table 1). The coefficients of variation for the measured traits varied between 49.65% and 146.60% under alkali stress, compared with 17.71–94.71% in the control (CK). Under alkali treatment, PH, RL, SD and FW were reduced compared with CK, suggesting that alkali stress suppressed shoot and root growth of potato. Meanwhile, Pro contents, POD and SOD activities increased markedly compared to CK, implying that alkali stress profoundly modulated osmotic adjustment and oxidative response pathways in potato.

Table 1. Physiological and biochemical parameters of potato accessions under alkali stress.

Treatment	Index	Min	Max	Mean	SD[1]	CV (%)
CK	PH (cm)	4.53	13.89	8.30	2.61	31.45
	RL (cm)	2.26	18.83	11.40	5.04	44.21
	SD (mm)	0.52	1.28	0.96	0.17	17.71
	FW(g)	0.09	0.61	0.32	0.12	37.50
	CAT (U/g)	571.85	1952.53	1098.66	343.38	31.25
	MDA (nmol/g)	4.84	92.20	24.45	22.72	92.94
	POD (U/g)	9349.20	81,129.30	32,150.13	20,179.11	62.77
	PRO (ug/g)	1.48	84.06	25.77	24.41	94.71
	SOD (U/g)	1559.50	26,897.11	11,842.15	7685.37	64.90
$NaHCO_3$	PH (cm)	0.00	4.83	2.86	1.42	49.65
	RL (cm)	0.00	7.46	2.00	2.25	112.50
	SD (mm)	0.00	1.13	0.73	0.37	50.68
	FW(g)	0.00	0.34	0.07	0.07	100.00
	CAT (U/g)	277.90	2421.55	639.73	93.44	93.44
	MDA (nmol/g)	4.09	37.12	14.81	8.77	59.18
	POD (U/g)	7203.00	98,886.90	46,933.83	28,498.82	60.72
	PRO (ug/g)	5.11	205.24	81.40	60.00	73.71
	SOD (U/g)	1983.97	10,7800.21	20,515.51	30,075.85	146.60

Note: CK: 17 potato accessions grown on MS solid medium; $NaHCO_3$: 17 potato accessions grown on MS solid medium supplemented with 10 mM $NaHCO_3$. SD[1]: standard deviation; CV: Coefficient of variation; PH: plant height; RL: root length; FW: fresh weight; SD: stem diameter; CAT: Catalase; MDA: Malondialdehyde; POD: Peroxidase; PRO: Proline; SOD: Superoxide dismutase. Completely dead plantlets were excluded from physiological measurements; only viable seedlings were sampled for enzyme activity determination.

3.2. Correlation Analysis and PCA of Potato Under Alkali Stress

Correlation analysis was conducted to assess the morphological and physiological traits of the 17 potato accessions under alkali stress (Figure 3). Under CK, PH was significantly positively correlated with RL, SD, FW, and POD, while CAT and SOD were negatively correlated with morphological indicators and positively correlated with other

physiological indicators. However, under alkali stress, PH was significantly negatively correlated with RL, SD, and FW, while CAT was positively correlated with morphological indicators. This indicates that alkali stress has a significant impact on catalase's effect on plant growth. Furthermore, the values of POD, PRO, and SOD under alkali stress treatment were significantly different from the control, further reflecting that alkali stress causes both oxidative damage and osmotic stress in plants. Simultaneously, plants enhance their resistance by upregulating antioxidant enzymes and osmotic regulators. Thus, single-trait evaluation is insufficient for accurate assessment of alkali tolerance in potato; multivariate statistical approaches integrating multiple parameters are required for comprehensive evaluation.

Using the eigenvalue > 1 criterion combined with the principal component loading matrix, PCA distilled nine morphological, physiological and biochemical traits into three uncorrelated composite indices, which accounted for 77.78% of the total variance (Table 2). PC1 primarily combined growth indicators such as FW and SD, and was named the growth factor; PC2 mainly integrated physiological indicators including PRO, SOD, and POD, and was designated as the antioxidant defense factor; PC3 was mainly characterized by plant height (PH), POD and MDA, representing shoot elongation coupled with oxidative stress responses. These results indicate that plant alkali tolerance is primarily influenced by the synergistic effects of biomass accumulation and the antioxidant enzyme system.

Table 2. Descriptive statistics of potato accessions under alkali stress.

Comprehensive Indicator	Eigen Value	Cumulative Contribution Rate (%)	Eigenvector								
			PH	RL	SD	FW	CAT	MDA	POD	PRO	SOD
PC1	3.30	36.66	−0.05	−0.06	0.32	0.42	0.30	0.19	−0.03	−0.12	−0.05
PC2	2.07	59.66	−0.06	−0.24	0.04	−0.11	−0.08	0.05	0.27	0.39	0.36
PC3	1.58	77.78	0.46	0.23	−0.31	−0.10	0.15	0.22	0.32	−0.02	0.02

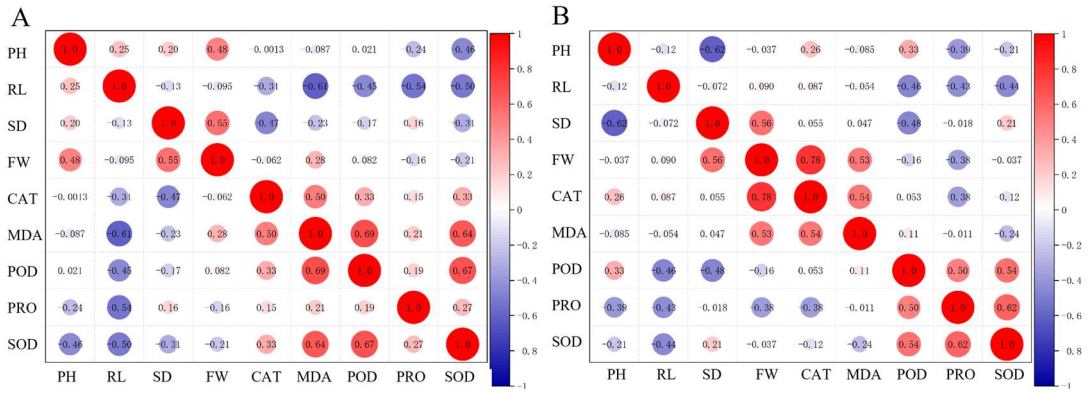


Figure 3. Correlation analysis of potato materials under alkali stress. (**A**) CK: correlation analysis of nine morphological, physiological and biochemical traits of 17 potato accessions grown on MS solid medium. (**B**) Correlation analysis of nine morphological, physiological and biochemical traits of 17 potato accessions grown on MS solid medium with 10 mM $NaHCO_3$. The circle size represents the absolute value of Pearson correlation coefficient.

3.3. Comprehensive Evaluation, Cluster Analysis and Regression Modeling for Alkali Tolerance in Potato

A value of the nine traits were computed using the established formulas for comprehensive alkali-tolerance evaluation of each potato accession. Z943 exhibited the highest A value, representing superior alkali tolerance, while Z440-1 had the minimum *A* value, which was indicative of weaker tolerance to alkali stress. Based on principal component analysis of potato alkali tolerance-related indicators, three core principal components with a cumulative contribution rate of 77.78% were extracted, and 17 potato accessions underwent systematic cluster analysis. The results showed that they could be divided into three groups (I–III) (Figure 4). Group I included four clonal lines: Z943, Z510-1, Z1219-1, and Z1074-1, which are alkali-tolerant potato accessions. Under alkali stress, this group exhibits high antioxidant enzyme activity and proline accumulation, low malondialdehyde content, and the lowest inhibition of growth indicators, making it the group with the best alkali tolerance among the tested materials. Group II includes nine clonal lines: Z1266-1, Z1268-1, Z1264-1, Z494, Z1045, Z456-2, Z1076-1, Z700-1, and Z1184-1, which are moderately alkali-tolerant. Group III includes Z965, Z1277-1, Z440-1, and Z850-1, which are alkali-sensitive potato accessions. The results of this cluster analysis are highly consistent with the conclusions of previous correlation and principal component analyses. The alkali-tolerant groups identified by the clusters can provide a scientific basis for screening potato alkali-tolerant breeding parents and promoting varieties suitable for alkali soils.

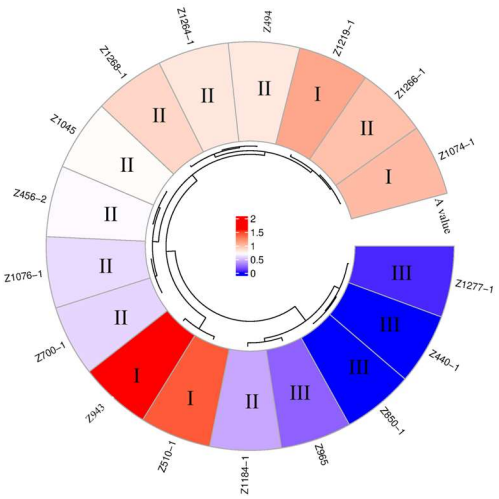


Figure 4. Cluster dendrogram of alkali tolerance indicators of 17 potato plantlets. A value represents the comprehensive alkali tolerance score calculated by membership function and PCA. The *A* value serves as the basis for plotting.

To comprehensively evaluate the alkali tolerance of other potato accessions, this study established a multiple linear regression model using stepwise regression analysis. The alkali-tolerance coefficients of nine morphological and physiological indicators were used as independent variables, and the comprehensive alkali-tolerance evaluation value A was used as the dependent variable. Redundant indicators that did not significantly contribute to alkali tolerance were gradually eliminated through stepwise regression. Finally, core predictors that significantly and independently contributed to potato alkali tolerance were selected, resulting in the linear regression equation $A = 0.790 - 0.124\ RL + 0.000276\ CAT$. Stepwise regression revealed that RL and CAT together explained 57.5% of

the variation in the comprehensive alkali tolerance score (A value): R^2 (coefficients of determination) = 0.516, F = 9.544, df_1 = 2, df_2 = 14, p = 0.002, n = 17. Diagnostic checks confirmed no obvious residual autocorrelation (Durbin–Watson = 1.577), and residuals approximately followed a normal distribution, verifying the validity of the regression model. The RL and CAT indicators are probably sensitive to alkali stress and can be used to evaluate the alkali tolerance of potatoes.

3.4. Quality Evaluation of Potato Transcriptome Data

To further investigate the alkali-tolerance mechanisms of alkali-tolerant potato accessions, alkali-tolerant (Z943) and -sensitive (Z965) potato accessions were treated with 10 mM $NaHCO_3$ at 0 h, 6 h, 12 h and 24 h. Roots were chosen because they are the primary organ directly perceiving bicarbonate alkali stress. Thus, the roots of Z943 and Z965 were collected for transcriptome sequencing analysis. Sequencing produced 1267.39 million raw reads. After filtering out low-quality reads and adapter sequences, 636.33 million and 655.34 million clean reads were retained for the two accessions, corresponding to 95.46 Gb and 98.32 Gb of sequencing data, respectively. The GC content ranged from 42.00% to 42.79%, and the mean Q30 value reached 96.14% (Table S3). Clean reads were aligned to the solanum tuberosum reference genome v6.1, with mapping rates between 87.48% and 89.04% (Table S4). Pearson's correlation coefficients among the three biological replicates of each sample varied from 0.710 to 0.994 (Figure S1), demonstrating consistent gene expression profiles within replicates. Collectively, these data confirmed that the sequencing depth and quality were adequate for subsequent transcriptome analysis.

3.5. Identification of Differentially Expressed Genes

The DEG profiles of the two potato accessions (Z943 and Z965) exposed to $NaHCO_3$ stress for 6, 12, and 24 h are shown in Figure 5A. Venn analysis of differentially expressed genes (DEGs) was performed for the alkali-tolerant line Z943 and alkali-sensitive line Z965 after $NaHCO_3$ treatment for 6, 12, and 24 h (Table S5). At 6 h, 1514 and 1041 DEGs were uniquely identified in Z943 and Z965, respectively, with 623 DEGs shared by both genotypes. At 12 h, the number of unique DEGs increased to 2977 in Z943 but decreased to 602 in Z965, and only 375 DEGs were common to both lines. At 24 h, DEG numbers increased markedly in both genotypes: Z943 had 5680 unique DEGs and Z965 had 1397 unique DEGs, with 1283 shared DEGs. Overall, Z943 activated substantially more DEGs than Z965 as the stress duration extended, suggesting that the tolerant genotype triggers a broader transcriptional reprogramming under prolonged alkali stress. Across all comparison combinations, the total number of DEGs peaked at 24 h under alkali stress. At this time point, the alkali-tolerant line Z943 had far more DEGs (6963) than the sensitive line Z965 (2680), indicating that 24 h represents a critical time point for the transcriptional response of potato to alkali stress. DEGs were screened using edgeR (version 3.22.5) with a threshold of $|\log2 \text{ (fold change)}| \geq 1$ and an adjusted p-value < 0.05. PCA showed significant separation between the alkali-resistant and -sensitive samples, indicating that alkali stress was the dominant factor causing transcriptome variation (Figure 5B).

Therefore, we compared the DEGs of Z943 and Z965 under control (CK) and 24 h alkali treatment, and identified a total of 1283 DEGs involved in the alkali stress response (Figure 5C). Based on the expression levels of these DEGs (log2FPKM+1), centered and normalized, cluster analysis was performed, and four cluster line charts with distinct expression patterns were obtained (Figure 5D). Among them, the genes in cluster line charts 1 and 2 showed markedly higher expression after 24 h alkali treatment than under CK; in cluster line chart 2, the expression of Z943 was significantly higher than that of Z965. In contrast, the genes in cluster line chart 3 showed higher expression under CK than after 24 h alkali treatment; in cluster line chart 4, the expression of Z965 was markedly

higher than that of Z943. Therefore, we selected a total of 716 DEGs from clusters 1 and 2 as alkali stress-related genes for subsequent analysis.

To further analyze the core DEGs involved in the potato response to alkali stress, a consensus network was constructed using WGCNA. Eight modules significantly associated with alkali stress were identified (Figure 6), along with the core genes within each module (Table S6). The genes within the core modules identified via WGCNA were then compared with the DEGs obtained from the Z943_24h vs. Z943_CK and Z965_24h vs. Z965_CK comparisons. Ten overlapping genes potentially associated with alkali tolerance were identified, providing a basis for future research on this topic.

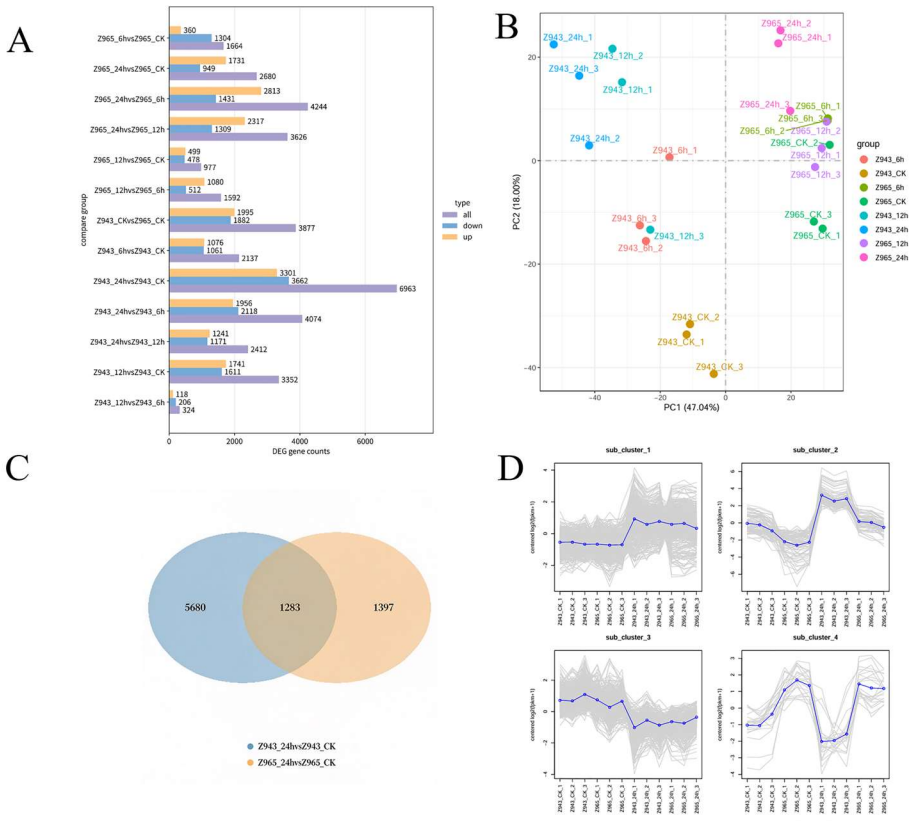


Figure 5. Analysis of DEGs. (**A**): The number of genes expressed in Z943 and Z965. (**B**): PCA between the alkali-resistant and -sensitive samples. (**C**): Venn diagram of DEGs in 943 and 965 after 24 h of alkali treatment. (**D**): Cluster line charts of DEGs, sample names are plotted on the x-axis, and the y-axis corresponds to log-centered normalized expression values. In each subplot, each gray line depicts the relative corrected expression level of a single gene in the given cluster under various experimental conditions. The blue line represents the mean expression profile of all genes belonging to this cluster across experimental treatments.

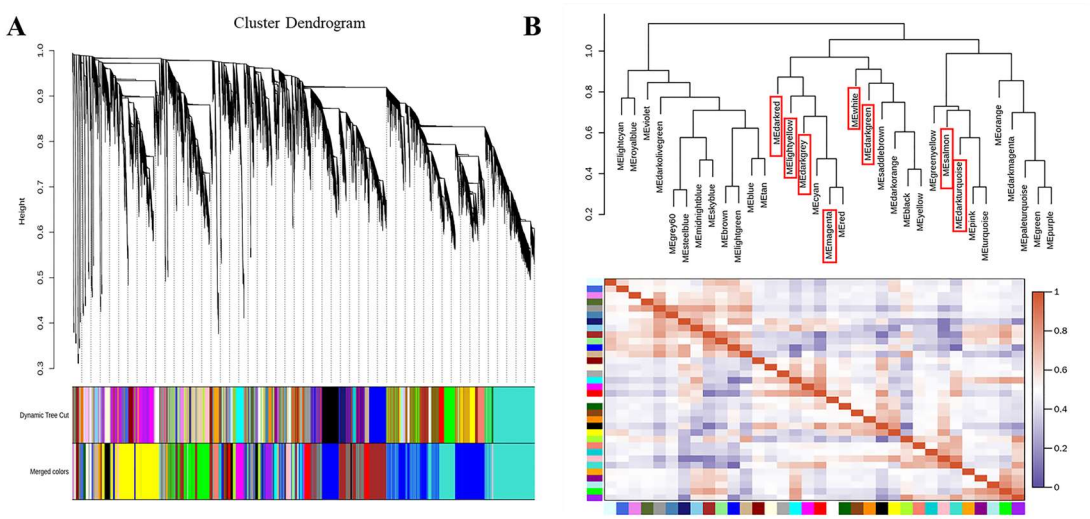


Figure 6. Co-expression network analysis of DEGs. (**A**): Co-expression network analysis identifying gene modules associated with potato alkali stress responses under different treatment conditions. (**B**): Inter-module correlation heat maps. Red frames represent modules related to alkali stress.

3.6. GO Functional Annotation and KEGG Analysis of DEGs

According to the GO enrichment results, these DEGs were mainly enriched in nine GO terms, including "oxidoreductase activity, acting on peroxide as acceptor (GO:0016684)", "endopeptidase inhibitor activity (GO:0004866)", and "peroxidase activity (GO:0004601)". These results demonstrated that, following 24 h of alkali treatment, potato responds to alkali stress by modulating peroxidase and oxidoreductase activities to scavenge reactive oxygen species, as well as through the protein degradation pathway mediated by endopeptidases. KEGG pathway enrichment revealed that the DEGs were predominantly enriched in "biosynthesis of secondary metabolites" (sot01110), "Metabolic pathways" (sot01100) and "Phenylpropanoid biosynthesis" (sot00940). The top 20 enriched GO terms and KEGG pathways are shown in Figure 7. These pathways play important roles in the regulation of alkali tolerance in potato.

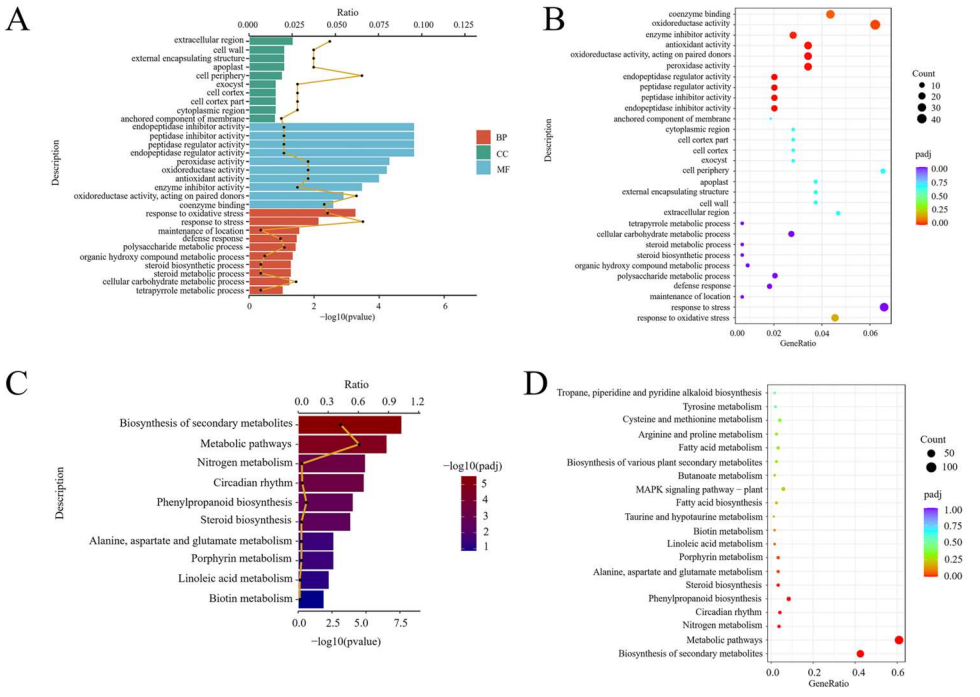


Figure 7. GO and KEGG enrichment analysis of DEGs. (**A**,**B**): GO enrichment analysis histogram and GO enrichment analysis scatter plot. (**C**,**D**): KEGG enrichment analysis histogram and KEGG enrichment analysis scatter plot.

3.7. Screening and Validating Genes Related to the Alkali-Stress Responses in Potato via qRT-PCR

To facilitate more precise screening of candidate genes, DEGs were compared with the genes in the significantly enriched GO and KEGG pathways. First, the genes in pathways were compared with the DEGs from Z943_24h vs. Z943_CK and Z965_24h vs. Z965_CK, and 74 overlapping genes were identified. Subsequently, the DEG analysis was combined with the WGCNA results: the 10 overlapping DEGs screened by WGCNA were merged with the 8 module key genes and filtered in combination with the differential expression analysis, ultimately yielding 92 candidate DEGs related to alkali tolerance (Table S7). To validate the expression patterns of key pathway genes associated with alkali tolerance in potato, we selected 12 candidate genes involved in phenylpropanoid biosynthesis, biosynthesis of secondary metabolites, and oxidoreductase activity for qRT-PCR analysis. Key genes were found to be significantly up-regulated after 24 h of alkali stress, which was consistent with the RNA-seq results (Figure 8). These findings confirmed the accuracy of the transcriptome data and indicated that these pathways play important regulatory roles in the response of potato to alkali stress.

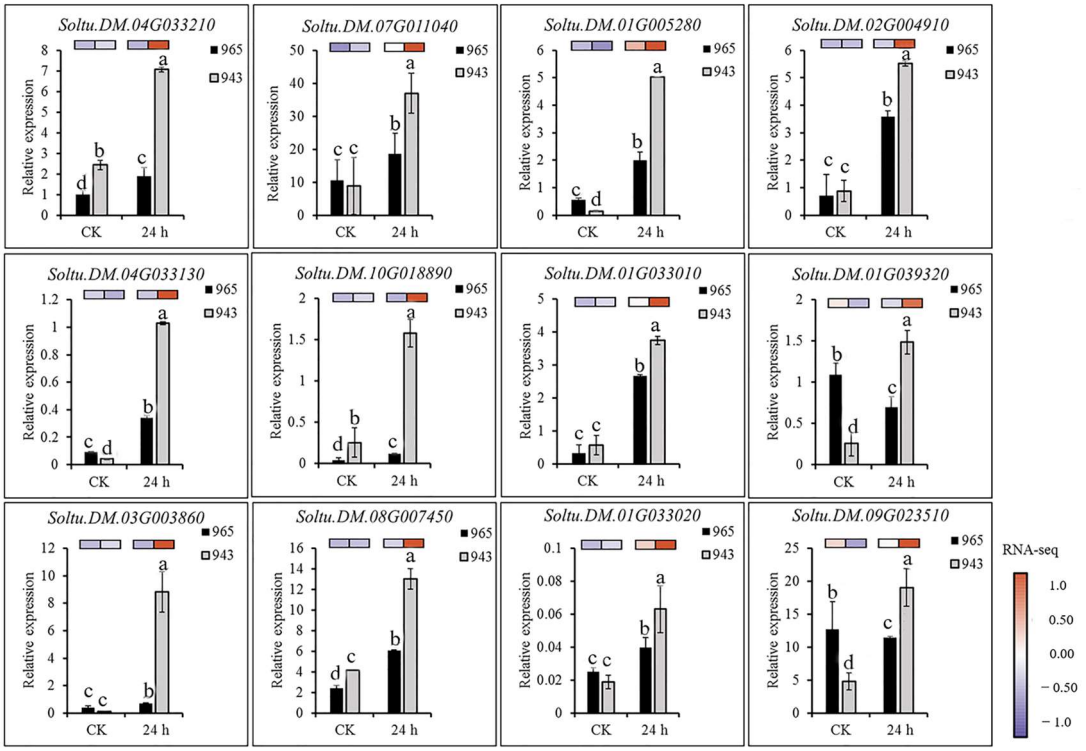


Figure 8. qRT-PCR analysis of DEGs in potato roots under alkali stress. CK: the expression levels of DEGs in 965 and 943 when grown in standard liquid MS medium; 24 h: the expression levels of DEGs in 965 and 943 after 24 h of cultivation in alkali liquid MS medium (containing 10 mM $NaHCO_3$, pH 8.2). The different lowercase letters above the bars mark significant differences ($p \leq 0.05$); the error bars show standard deviation.

4. Discussion

4.1. Potato Seedlings' Responses to Gradient $NaHCO_3$ Stress and Limitations of the In Vitro Assay System

This study systematically analyzed the growth and physiological responses of potatoes under gradient $NaHCO_3$ alkali stress; determined the optimal stress threshold for alkali-tolerance identification; and provided phenotypic evidence for subsequent transcriptomic analysis of the molecular mechanisms of alkali adaptation. The results showed that low-concentration $NaHCO_3$ stress exerted no obvious inhibitory effects on potato growth and development, whereas high-level alkali stress markedly retarded plant growth, accompanied by significant reductions in plant height, fresh weight, stem diameter and root activity. This response pattern is consistent with previous reports on alkali stress in other crop species [1,51–53], confirming that potato exhibits a prominent concentration-dependent effect in response to alkali stress. Gradient stress treatments were employed in this study, with concentration parameters optimized based on the literature and preliminary experiments. The in vitro system eliminates environmental noise associated with field conditions; it allows for the stable capture of stress phenotypes while avoiding plant lethality and non-specific physiological toxicity caused by extreme stress, thus ensuring the reliability of the phenotypic and physiological data analysis.

It should be noted that MDA content and CAT activity decreased under $NaHCO_3$ stress, which differs from the commonly reported pattern in many plant species [22]. This unexpected response may be partly attributed to the specific stress conditions of our in vitro system, including the unbuffered culture medium and sampling time point. It is possible that certain potato genotypes activate distinct regulatory pathways to alleviate oxidative injury at the assayed timepoint, thereby reducing MDA accumulation and the requirement for high CAT activity. Such variable responses indicate that MDA-based oxidative signals should be interpreted cautiously when evaluating the alkali responses of potato seedlings [11,54]. Further sampling across additional timepoints and stress concentrations will be required to clarify the dynamic changes in oxidative indicators under alkali stress.

In addition, the medium pH at the end of the 21-day treatment was not determined in this study, and pH may drift during seedling growth in this unbuffered MS system [55]. Accordingly, the phenotypic and molecular alterations observed here represent integrated responses to the combined effects of bicarbonate and the elevated initial pH induced by $NaHCO_3$, and further experiments with pH-matched controls without bicarbonate will help to disentangle the independent effects of high pH and bicarbonate on potato seedlings [4]. Moreover, the phenotypic and physiological assessments were performed on solid medium after 21 days of alkali stress, whereas transcriptome sampling was conducted on seedlings grown in liquid culture at 0–24 h. Since we did not characterize the phenotypic differences between Z943 and Z965 under the liquid-culture system, we cannot fully confirm whether the two genotypes maintain a consistent alkali tolerance divergence across these two culture systems.

This experimental setup cannot fully recapitulate the complex physicochemical and biological properties of natural alkali soils, including heterogeneous ion distribution, rhizosphere interactions, and dynamic water and nutrient cycles. Consequently, the conclusions drawn from this in vitro assay are preliminary [12]. Further investigations involving liquid-culture phenotyping, pot experiments and field trials under representative alkali conditions are essential, as it is necessary to verify the alkali tolerance performance of these materials before they can be considered for practical cultivation and breeding applications.

4.2. Multivariate Statistical Evaluation of Alkali Tolerance in Potato

Comprehensive evaluation of potato alkali tolerance cannot be objectively achieved using a single trait, and multi-index datasets commonly contain redundant information, necessitating multivariate statistical analysis [28,56–58]. Correlation analysis revealed significant associations among physiological indicators, demonstrating that alkali tolerance in potato is a complex trait co-regulated by multiple factors. PCA reduced the dimensionality of original variables to effectively discriminate potato genotypes with divergent alkali tolerance [11,28,59]. Combined with membership function and cluster analysis, the tested accessions were classified into alkali-tolerant, intermediate and sensitive groups, directly reflecting the genetic differentiation of alkali tolerance. Stepwise regression further screened core indicators for rapid tolerance evaluation and established a predictive model, offering a feasible strategy for high-throughput primary screening of alkali-tolerant potato germplasms [42,60,61]. Although the in vitro tissue culture phenotyping system is easy to operate, phenotypes only represent the external manifestation of genotypes under alkali stress. The molecular regulatory network underlying genotypic differences in alkali tolerance remains to be deciphered by transcriptomic profiling of differentially expressed genes.

4.3. The Regulatory Mechanisms Underlying Alkali Stress via DEG-Enriching Pathways

Transcriptome sequencing was used to obtain the gene expression profiles of potato tissue-culture plantlets under alkali stress. DEGs indicated that pathways such as phenylpropanoid biosynthesis, secondary metabolite biosynthesis, peroxidase activity, and oxidoreductase activity play key roles in the response to alkali stress. Studies have shown that under alkali stress, the expression of key enzyme genes phenylalanine ammonia-lyase (PAL) and cinnamate 4-hydroxylase (C4H) in the phenylpropanoid biosynthesis pathway is significantly upregulated, and effectively drives the synthesis of protective metabolites such as lignin, phenolic acids and flavonoids [62]. Multi-omics analysis of rice alkali tolerance identified the phenylpropanoid biosynthesis pathway as the primary pathway associated with the response to $NaHCO_3$ stress. It promotes the accumulation of phenolic antioxidants and lignin precursors, and enhances reactive oxygen species (ROS) scavenging capacity and cell wall reinforcement, thereby improving adaptability to $NaHCO_3$ stress [63].

In this study, several candidate genes in the phenylpropanoid biosynthesis pathway (sot00940) were identified as potential regulators of the alkali stress response in potato (Figure S2). Among them, *Soltu.DM.05G019180* encodes C4H, a core enzyme that catalyzes the conversion of cinnamic acid to p-coumaric acid and supplies precursors for downstream lignin and phenolic acid biosynthesis. Its expression changes under alkali stress may alter metabolic flux, thereby affecting cell wall lignification and antioxidant accumulation. In addition, *Soltu.DM.01G001850*, *Soltu.DM.04G036980*, and *Soltu.DM.11G011560* encode POD, which participate in both lignin polymerization and ROS scavenging, suggesting a dual role in cell wall reinforcement and oxidative stress defense. The remaining candidates, such as *Soltu.DM.09G023510*, are either annotated as α/β-hydrolase superfamily proteins or remain functionally uncharacterized. Although their roles are unclear, they may be involved in phenolic ester hydrolysis or metabolite modification. Overall, these findings suggest that potato may enhance alkali tolerance through C4H-mediated phenylpropanoid flux combined with POD-mediated lignin deposition and ROS detoxification. Nevertheless, we cannot rule out the possibility that the activated phenylpropanoid pathway also contributes to iron mobilization via coumarin synthesis under bicarbonate stress [64]. Further transcriptomic and transgenic analyses are needed to confirm the functions of these candidate genes.

We also found that *Soltu.DM.07G014440*, *Soltu.DM.03G003860* and *Soltu.DM.09G023510* jointly participate in the secondary metabolic and phenylpropanoid

biosynthesis pathways, cooperatively mediating potato adaptation to alkali stress (Figure S3). Alkali stress activates key secondary metabolic enzyme genes and induces protective metabolite accumulation, alleviating ion toxicity and oxidative damage through structural protection and antioxidant detoxification [23,65], which indicates that alkali tolerance in potato is a polygenic quantitative trait regulated by morphological, physiological, and multiple core metabolic pathways [66–68]. Meanwhile, oxidoreductases exhibited significant differential expression by regulating the activities of classic antioxidant enzymes such as SOD, POD, and CAT. They maintain intracellular redox homeostasis and mitigate membrane lipid peroxidation damage caused by the excessive accumulation of ROS [69–72]. These transcriptomic findings align closely with the previously determined physiological phenotypes of antioxidant enzymes, providing mutual corroboration at both the physiological and molecular levels (Table 1).

Integrating phenotypic characterization, multivariate statistical analysis, and transcriptome sequencing, this study identified candidate genes responsive to alkali stress, providing germplasm and genetic resources for mechanistic elucidation and molecular breeding. However, as stress treatments and phenotypic assessments were performed under controlled in vitro conditions, future pot and field trials in alkali soils are needed. For functional validation of candidate alkali-tolerance genes, potato genetic transformation efficiency is strongly genotype-dependent, and large differences are commonly observed across cultivars [73–75]. In the present study, Z943 and Z965 were selected as the experimental materials. We are currently optimizing the genetic transformation system for these two genotypes, and the biological functions of the identified DEGs will be characterized in follow-up experiments.

4.4. Key Alkali Stress-Responsive Genes Identified by Transcriptome and WGCNA Analyses

Integrated transcriptomic and WGCNA analyses identified eight core alkali-responsive hub genes (Table S6) which are enriched in plant abiotic stress response pathways and form interconnected gene modules to synergistically maintain plant physiological homeostasis under alkali stress. Among them, *Soltu.DM.11G023490* regulates the catalytic activity of aldehyde oxidase and mediates phytohormone signaling under alkali conditions. Previous studies have shown that aldehyde oxidase 2 contributes to abscisic acid biosynthesis, plant defense, and alkali tolerance [76]. *Soltu.DM.08G015830* encodes 3-ketoacyl-CoA synthase (KCS). Previous studies have confirmed that members of the KCS gene family possess β-ketoacyl-CoA synthase catalytic functions and are involved in hormone signal transduction, defense responses, and the regulation of resistance to multiple abiotic stresses [77,78]. *Soltu.DM.06G019060* is associated with the activity of cytochrome P45071D7. The expression dynamics of cytochrome P450 family genes participate in signal transduction and stress regulatory networks in response to alkali stress [60,79,80]. These genes are associated with alkali tolerance, and they provide a valuable resource for future functional validation.

5. Conclusions

In summary, 10 mM $NaHCO_3$ was determined as the optimal concentration for inducing alkali stress in potato. The morphological and physiological traits of 17 accessions were evaluated using multivariate methods, including principal component, membership function, and cluster analyses, yielding a linear regression model ($A = 0.790 - 0.124\ RL + 0.000276\ CAT$). Transcriptomic analysis of alkali-tolerant and -sensitive accessions identified 1283 DEGs that responded to alkali stress, which were enriched in peroxidase activity, as well as phenylpropanoid biosynthesis. Combined hierarchical clustering and WGCNA identified 92 candidate genes, while 12 DEGs were validated by qRT-PCR, consistent with the transcriptomic data. These findings facilitate the screening

of alkali-tolerant potato accessions and provide a resource for functional characterization of alkali stress genes and future breeding.

Supplementary Materials: The following supporting information can be downloaded at: https://www.mdpi.com/article/10.3390/agronomy16232419/s1, Figure S1: Heatmap of correlations between samples; Figure S2: KEGG pathway map of phenylpropanoid biosynthesis; Figure S3: Overview of KEGG metabolic pathways (map01100); Table S1: Potato varieties and germplasms used for alkali tolerance assessment; Table S2: Gene IDs and primer sequences for the genes used for qPCR verification; Table S3: Statistics of the sequencing for potato transcriptome; Table S4: The results of sequencing data mapped to the reference genome; Table S5. Numbers of unique, shared and total DEGs in Z943 and Z965 under $NaHCO_3$ stress at different time points; Table S6: DEGs and hub gene of different modules; Table S7: Candidate differentially expressed genes and annotations.

Author Contributions: X.Z. and S.Z. jointly designed the research, analyzed the RNA-seq and drafted the original manuscript. C.L. performed and analyzed qRT-PCR data. S.Z., H.W., H.Z., Z.L. and J.X. performed experiments to measure morphological and physiological indices. X.Z., R.Y., S.L. and P.G. performed data analysis. Q.C. and L.H. conceived the research, supervised the whole study, revised the manuscript, and acquired the funding. All authors have read and agreed to the published version of the manuscript.

Funding: This research was funded by the National Natural Science Foundation of China (32000199); the Natural Science Foundation of Shandong of China (ZR2025MS297); the Project of Shandong Province Higher Educational Science and Technology Program (2023KJ270); the Shandong Province Higher Educational Science and Technology Program (2024KJG070).

Data Availability Statement: The raw transcriptomic sequence data generated in this study have been deposited in the NCBI Sequence Read Archive (SRA) under BioProject accession number PRJNA1540394. The BioProject is accessible at the following URL: https://www.ncbi.nlm.nih.gov/bioproject/PRJNA1540394 (accessed on 6 October 2026).

Acknowledgments: We thank Leling Xisen Potato Industry Group Co., Ltd. (Leling, Dezhou, Shandong, China) for providing the seedlings of 17 potato materials.

Conflicts of Interest: The authors declare no conflicts of interest.

Abbreviations

The following abbreviations are used in this manuscript:

ABA	Abscisic Acid
CAT	Catalase
CV	Coefficient of variation
DEGs	Differentially expressed genes
FPKM	Fragments Per Kilobase of exon model per Million mapped fragments
FW	Fresh weight
GO	Gene Ontology
KEGG	Kyoto Encyclopedia of Genes and Genomes
MDA	Malondialdehyde
PCA	Principal component analysis
PH	Plant height
POD	Peroxidase
PRO	Proline
qRT-PCR	Quantitative real-time PCR
RL	Root length
RNA-Seq	RNA sequencing
ROS	Reactive oxygen species

SD[1]	Standard deviation
SD	Stem diameter
SOD	Superoxide dismutase
WGCNA	Weighted correlation network analysis
pH	Potential of hydrogen

References

1. Yang, S.; Xu, Y.; Tang, Z.; Jin, S.; Yang, S. The Impact of Alkali Stress on Plant Growth and Its Alkali Resistance Mechanisms. *Int. J. Mol. Sci.* **2024**, *25*, 13719. https://doi.org/10.3390/ijms252413719.
2. Wei, Y.; Liu, Q.; Zhang, J.; Ren, M.; Luo, X. Transforming barriers into opportunities: Saline-alkali-tolerant plants for sustainable agriculture expansion. *J. Agric. Food Chem.* **2025**, *73*, 32430–32449. https://doi.org/10.1021/acs.jafc.5c10327.
3. Xu, J.; Chen, Q.; Liu, P.; Jia, W.; Chen, Z.; Xu, Z. Integration of mRNA and miRNA Analysis Reveals the Molecular Mechanism Underlying Salt and Alkali Stress Tolerance in Tobacco. *Int. J. Mol. Sci.* **2019**, *20*, 2391. https://doi.org/10.3390/ijms20102391.
4. Li, J.; Yang, Y. How do plants maintain pH and ion homeostasis under saline-alkali stress? *Front. Plant Sci.* **2023**, *14*, 1217193. https://doi.org/10.3389/fpls.2023.1217193.
5. Colmer, T.; Munns, R.; Flowers, T. Improving salt tolerance of wheat and barley: Future prospects. *Aust. J. Exp. Agric.* **2005**, *45*, 1425–1443. https://doi.org/10.1071/EA04162.
6. Khan, M.; Karim, M.; Haque, M.; Islam, M.; Karim, A.; Mian, M. Influence of Salt and Water Stress on Growth and Yield of Soybean Genotypes. *Pertanika J. Trop. Agric. Sci.* **2016**, *39*, 167.
7. Dong, T.; Yan, L.; Wang, J.; Niu, Y.; Wang, L. Salt tolerance in soybean (*Glycine max* L.): A comprehensive review of molecular mechanisms, key regulators, and future perspectives for saline soil utilization. *Plants* **2025**, *14*, 3668. https://doi.org/10.3390/plants14233668.
8. Wang, X.; Song, J.; Fan, W.; He, Z.; Zhang, X. Evaluation of comprehensive alkali resistance in tomato germplasm seedlings. *Euphytica* **2025**, *221*, 137. https://doi.org/10.1007/s10681-025-03585-6.
9. Ren, S.; Tan, J.; Zhou, S.; Sun, H.; Li, H.; Li, W.; Li, N.; Wu, J.; Ren, X.; Ci, J.; et al. Germplasm Selection and Comprehensive Evaluation of Maize Inbred Lines at Germination and Seedling Stage for Saline-Alkali Tolerance. *Agronomy* **2025**, *15*, 626. https://doi.org/10.3390/agronomy15030626.
10. Chen, S.; Li, Y.; Zhang, W.; Shen, H.; Wang, S.; Wang, R.; Li, H. Evaluation of Saline-Alkali Tolerance of *Oenothera* L. Germplasms and Their Morpho-Physiological Responses to Saline-Alkali Stress. *Physiol. Plant.* **2025**, *177*, e70541. https://doi.org/10.1111/ppl.70541.
11. Yang, X.; Liu, Z.; Chen, J.; Zhang, W.; Yang, W.; Shen, C.; Kang, Y.; Qin, S. PP2C-Mediated ABA Signaling Pathway Underlies Exogenous Abscisic Acid-Induced Enhancement of Saline-Alkali Tolerance in Potato (*Solanum tuberosum* L.). *Plants* **2025**, *14*, 1921. https://doi.org/10.3390/plants14131921.
12. Han, X.; Yang, R.; Zhang, L.; Wei, Q.; Zhang, Y.; Wang, Y.; Shi, Y. A Review of Potato Salt Tolerance. *Int. J. Mol. Sci.* **2023**, *24*, 10726. https://doi.org/10.3390/ijms241310726.
13. Dong, X.; Sui, C.; Wang, K.; Chen, W.; Li, Y.; Kear, P.J.; Chang, S.; Lv, D.; Jian, H. Melatonin enhances salt tolerance by inducing StMYB55 to improve flavonoid accumulation in potato. *Plant Physiol.* **2026**, *201*, kiag168. https://doi.org/10.1093/plphys/kiag168.
14. Chourasia, K.N.; Lal, M.K.; Tiwari, R.K.; Dev, D.; Kardile, H.B.; Patil, V.U.; Kumar, A.; Vanishree, G.; Kumar, D.; Bhardwaj, V.; et al. Salinity Stress in Potato: Understanding Physiological, Biochemical and Molecular Responses. *Life* **2021**, *11*, 545. https://doi.org/10.3390/life11060545.
15. Zhu, X.; Majeed, Y.; Duan, X.; Wang, K.; Duan, H.; Luo, J.; Guan, N.; Zheng, H.; Jin, H.; Chen, Z.; et al. Functional analysis of *StMAPK19* gene in response to salt stress in potato (*Solanum tuberosum* L.). *BMC Plant Biol.* **2025**, *25*, 1561. https://doi.org/10.1186/s12870-025-07434-5.
16. Wang, K.; Zhang, H.; Yang, L.; Wei, H.; Tang, X.; Zhang, N.; Si, H. *StMAPKK1* enhances drought and salt tolerance in potato via ROS scavenging and stomatal closure. *Plant Physiol. Biochem.* **2025**, *229*, 110383. https://doi.org/10.1016/j.plaphy.2025.110383.
17. Liu, S.; Wang, Y.; Wang, J.; Peng, R.; Cai, C.; Yan, L.; Lai, X. Overexpression of StBIN2 Improves Salt Stress Tolerance in Potato. *Int. J. Mol. Sci.* **2026**, *27*, 7747. https://doi.org/10.3390/ijms27177747.
18. Zhang, R.; Wang, Y.; Wang, X.; Jiao, S.; Lu, Y.; Du, Y.; Zhang, W.; Kang, Y.; Liu, Y.; Qin, S. Differential responses of microstructure, antioxidant defense, and plant hormone signaling regulation in potato (*Solanum tuberosum* L.) under drought, alkali salt, and combined stresses. *Sci. Hortic.* **2025**, *341*, 114014. https://doi.org/10.1016/j.scienta.2025.114014.

19. Wang, Y.; Zhang, R.; Wang, X.; Jiao, S.; Zhang, W.; Kang, Y.; Li, M.; Xie, J.; Yang, X.; Liu, Y. 24-epibrassinolide improves potato (*Solanum tuberosum* L.) tolerance to alkali salt stress by regulating antioxidant defence and photosynthetic properties. *J. Agron. Crop Sci.* **2025**, *211*, e70022. https://doi.org/10.1111/jac.70022.
20. Wang, J.; Wang, Y.; Lu, Y.; Wang, X.; Du, Y.; Zhang, W.; Kang, Y.; Qin, S. Identification and Expression Analysis of the Potato (Solanum tuberosum L.) stu-miR482 Family Under Exogenous 24-Epibrassinolide Treatments and Alkali Salt Stress. *Plants* **2026**, *15*, 1856. https://doi.org/10.3390/plants15121856.
21. Jiao, S.; Hu, X.; Wang, Y.; Zhang, R.; Wang, X.; Lu, Y.; Zhang, W.; Liu, Y.; Qin, S.; Kang, Y. Molecular mechanisms of potato (*Solanum tuberosum* L.) transcription factor S*tbZIP1* in regulating saline-alkali stress response through enhanced antioxidant capacity. *Chem. Biol. Technol. Agric.* **2025**, *12*, 140. https://doi.org/10.1186/s40538-025-00861-4.
22. Kang, Y.; Yang, X.; Liu, Y.; Shi, M.; Zhang, W.; Fan, Y.; Yao, Y.; Zhang, J.; Qin, S. Integration of mRNA and miRNA analysis reveals the molecular mechanism of potato (*Solanum tuberosum* L.) response to alkali stress. *Int. J. Biol. Macromol.* **2021**, *182*, 938–949. https://doi.org/10.1016/j.ijbiomac.2021.04.094.
23. Fu, Y.; Wang, Q.; Ge, Y.; Liao, H.; Yan, C. Exogenous spermidine (Spd) improves the tolerance to alkali-salt stress in potato. *BMC Plant Biol.* **2026**, *26*, 1568. https://doi.org/10.1186/s12870-026-09656-7.
24. Zhang, A.; Liu, Q.; Du, X.; Xing, B.; Zhang, S.; Li, Y.; Hao, L.; Wei, Y.; Liu, Y.; Li, P.; et al. Tissue-Specific RNA-Seq Analysis of Cotton Roots' Response to Compound Saline-Alkali Stress and the Functional Validation of the Key Gene GhERF2. *Plants* **2025**, *14*, 756. https://doi.org/10.3390/plants14050756.
25. Wang, J.; Sun, X.; Wang, P.; Wu, S.; Wang, Y. Exploring Birch Salt Tolerance Using Gene Regulatory Network Highlighting Hormone Signaling, Reactive Oxygen Species Scavenging, and Ion Homeostasis. *Physiol. Plant.* **2025**, *177*, e70331. https://doi.org/10.1111/ppl.70331.
26. Gubaidullin, N.; Ospankulova, G.; Gajimuradova, A.; Syzdykova, A.; Zhumalin, A.; Dairova, K.; Konysbayeva, D.; Gorbulya, V.; Makangali, K. ROS-Centered Transcriptomic Regulatory Networks Linking Salinity Stress, Antioxidant Defense and Processability Traits in *Salicornia* spp. *Curr. Issues Mol. Biol.* **2026**, *48*, 719. https://doi.org/10.3390/cimb48070719.
27. Zhang, J.; Hu, X.; He, S.; Liu, G.; Jiang, Z.; Zhang, D. Integrated physiological and transcriptomic analyses reveal the mechanisms of exogenous selenium-mediated alleviation of saline-alkali stress in tomato seedlings. *BMC Plant Biol.* **2026**. https://doi.org/10.1186/s12870-026-09927-3.
28. Zhao, P.; Chen, G.-X.; Zhang, Y.-P.; Yang, X.-H.; Liu, F.; Dong, D.-F. Alkali tolerance identification method of potato seedlings and comprehensive assessment of alkali tolerance of 86 kinds of potato germplasms. Acta Agron. Sin. 2025, 49, 2923–2934. https://doi.org/10.3724/sp.J.1006.2023.24278.
29. Wei, J.; Zhang, N.; Deng, Y.; Liu, S.; Yang, L.; Wang, X.; Wen, R.; Si, H. Functional analysis of the *StERF79* gene in response to drought stress in potato (*Solanum tuberosum* L.). *BMC Plant Biol.* **2025**, *25*, 387. https://doi.org/10.1186/s12870-025-06417-w.
30. Daud, M.; Li, W.; Qiao, H.; Adil, M.; Ashraf, M.A.; Khan, M.; Ijaz, H.; Haq, Z.u.; Bibi, N.; Xu, S. Assessment of Alfalfa varieties under salt stress through morpho-physiological and biochemical traits using a comprehensive membership function approach. *BMC Plant Biol.* **2026**, *26*, 1097. https://doi.org/10.1186/s12870-026-09157-7.
31. Shuxin, Z.; Zixuan, J.; Tao, F.; Yifan, L.; Wei, Z.; Rong, W.; Haichao, C.; Fangli, L.; Yaojun, Z.; Feihai, Y. Methods to evaluate plant tolerance to environmental stresses. *Biodivers. Sci.* **2025**, *33*, 24168. https://doi.org/10.17520/biods.2024168.
32. Zhang, W.; Yuan, S.; Liu, N.; Zhang, H.; Zhang, Y. Evaluation and screening of dwarfing 'Duli' (Pyrus betulifolia Bunge) seedlings by principal component analysis and membership function analysis. *Sci. Hortic.* **2025**, *345*, 114128. https://doi.org/10.1016/j.scienta.2025.114128.
33. Zhang, C.; Jiang, K.; Liu, Q.; Xu, H.; Ning, K.; Yu, H.t.; Zhang, M.; Zhu, J.; Chen, M. Screening of salt-tolerant soybean germplasm and study of salt-tolerance mechanism. *Plant Cell Rep.* **2025**, *44*, 187. https://doi.org/10.1007/s00299-025-03574-y.
34. Khadka, K.; Earl, H.J.; Raizada, M.N.; Navabi, A. A Physio-Morphological Trait-Based Approach for Breeding Drought Tolerant Wheat. *Front. Plant Sci.* **2020**, *11*, 715. https://doi.org/10.3389/fpls.2020.00715.
35. Rahman, S.U.; Han, J.C.; Yasin, G.; Imtiaz, M.T.; Zhao, X.; Alharbi, S.A.; Alfarraj, S.; Alarfaj, A.A. Synergetic effects of potassium and biochar on morphological, physiological, and biochemical attributes of maize crop grown under different levels of drought stress. *BMC Plant Biol.* **2025**, *25*, 402. https://doi.org/10.1186/s12870-025-06391-3.
36. Schneider, C.A.; Rasband, W.S.; Eliceiri, K.W. NIH Image to ImageJ: 25 years of image analysis. *Nat. Methods* **2012**, *9*, 671–675. https://doi.org/10.1038/nmeth.2089.
37. Giannopolitis, C.N.; Ries, S.K. Superoxide dismutases: I. Occurrence in higher plants. *Plant Physiol.* **1977**, *59*, 309–314. https://doi.org/10.1104/pp.59.2.309.

38. Maehly, A.C. The assay of catalases and peroxidases. *Methods Biochem. Anal* **1954**, *1*, 357–408. https://doi.org/10.1002/9780470110171.ch14.
39. Aebi, H. [13] Catalase in vitro. *Methods Enzymol.* **1984**, *105*, 121–126. https://doi.org/10.1016/S0076-6879(84)05016-3.
40. Heath, R.L.; Packer, L. Photoperoxidation in isolated chloroplasts: I. Kinetics and stoichiometry of fatty acid peroxidation. *Arch. Biochem. Biophys.* **1968**, *125*, 189–198. https://doi.org/10.1016/0003-9861(68)90654-1.
41. Bates, L.S.; Waldren, R.P.; Teare, I.D. Rapid determination of free proline for water-stress studies. *Plant Soil* **1973**, *39*, 205–207. https://doi.org/10.1007/BF00018060.
42. Lin, C.; Zheng, S.; Liu, K.; Yu, R.; Guan, P.; Hu, B.; Jiang, L.; Su, M.; Hu, G.; Chen, Q.; et al. Elucidating the molecular basis of salt tolerance in potatoes through miRNA expression and phenotypic analysis. *Sci. Rep.* **2025**, *15*, 2635. https://doi.org/10.1038/s41598-025-86276-5.
43. Chen, S.; Zhou, Y.; Chen, Y.; Gu, J. fastp: An ultra-fast all-in-one FASTQ preprocessor. *Bioinformatics* **2018**, *34*, i884–i890. https://doi.org/10.1093/bioinformatics/bty560.
44. Pham, G.M.; Hamilton, J.P.; Wood, J.C.; Burke, J.T.; Zhao, H.; Vaillancourt, B.; Ou, S.; Jiang, J.; Buell, C.R. Construction of a chromosome-scale long-read reference genome assembly for potato. *GigaScience* **2020**, *9*, Giaa100. https://doi.org/10.1093/gigascience/giaa100
45. Mortazavi, A.; Williams, B.A.; McCue, K.; Schaeffer, L.; Wold, B. Mapping and quantifying mammalian transcriptomes by RNA-Seq. *Nat. Methods* **2008**, *5*, 621–628. https://doi.org/10.1038/nmeth.1226.
46. Pertea, M.; Pertea, G.M.; Antonescu, C.M.; Chang, T.-C.; Mendell, J.T.; Salzberg, S.L. StringTie enables improved reconstruction of a transcriptome from RNA-seq reads. *Nat. Biotechnol.* **2015**, *33*, 290–295. https://doi.org/10.1038/nbt.3122.
47. Liao, Y.; Smyth, G.K.; Shi, W. featureCounts: An efficient general purpose program for assigning sequence reads to genomic features. *Bioinformatics* **2014**, *30*, 923–930. https://doi.org/10.1093/bioinformatics/btt656.
48. Robinson, M.D.; McCarthy, D.J.; Smyth, G.K. edgeR: A Bioconductor package for differential expression analysis of digital gene expression data. *Bioinformatics* **2010**, *26*, 139–140. https://doi.org/10.1093/bioinformatics/btp616.
49. Wu, T.; Hu, E.; Xu, S.; Chen, M.; Guo, P.; Dai, Z.; Feng, T.; Zhou, L.; Tang, W.; Zhan, L.; et al. clusterProfiler 4.0: A universal enrichment tool for interpreting omics data. *Innovation* **2021**, *2*, 100141. https://doi.org/10.1016/j.xinn.2021.100141.
50. Livak, K.J.; Schmittgen, T.D. Analysis of Relative Gene Expression Data Using Real-Time Quantitative PCR and the $2^{-\Delta\Delta CT}$ Method. *Methods* **2001**, *25*, 402–408. https://doi.org/10.1006/meth.2001.1262.
51. Fang, S.; Hou, X.; Liang, X. Response Mechanisms of Plants Under Saline-Alkali Stress. *Front. Plant Sci.* **2021**, *12*, 667458. https://doi.org/10.3389/fpls.2021.667458.
52. Dou, J.; Tang, Z.; Yu, J.; Wang, G.; An, W.; Zhang, Y.; Yang, Q. Effects of exogenous melatonin on the growth and photosynthetic characteristics of tomato seedlings under saline-alkali stress. *Sci. Rep.* **2025**, *15*, 5172. https://doi.org/10.1038/s41598-025-88565-5.
53. Guo, R.; Wang, X.; Ao, L.; Dai, X.; Zeng, C.; Zhang, H.; Wan, H. Effects of salt and alkali stress on seedling growth and main nutritional quality of rapeseed and pea. *Technol. Agron.* **2026**, *6*, e002. https://doi.org/10.48130/tia-0025-0015.
54. Hou, R.; Yang, L.; Wuyun, T.; Chen, S.; Zhang, L. Genes related to osmoregulation and antioxidation play important roles in the response of Trollius chinensis seedlings to saline-alkali stress. *Front. Plant Sci.* **2023**, *14*, 1080504. https://doi.org/10.3389/fpls.2023.1080504.
55. Chen, J.; Li, X.; Ye, X.; Guo, P.; Hu, Z.; Qi, G.; Cui, F.; Liu, S. An S-ribonuclease binding protein EBS1 and brassinolide signaling are specifically required for Arabidopsis tolerance to bicarbonate. *J. Exp. Bot.* **2021**, *72*, 1449–1459. https://doi.org/10.1093/jxb/eraa524.
56. Pan, Z.; Ge, Z.; Gao, F.; Ao, M.; Guan, Y. Comprehensive evaluation of maize germplasm for alkali tolerance during germination. *Front. Plant Sci.* **2026**, *16*, 1728607. https://doi.org/10.3389/fpls.2025.1728607.
57. Tian, Y.; Gao, Q.; Zhu, G.; Wang, C.; Hua, F.; Li, C.; Cao, P.; Gao, F.; Zhu, J. Evaluation of saline-alkali tolerance in 71 soybean germplasms based on multi-method integrated analysis at the germination stage. *PeerJ* **2026**, *14*, e21642. https://doi.org/10.7717/peerj.21642.
58. Zhang, F.; Zhao, L.; Guo, T.; Wang, Z.; Lou, P.; Li, J. Rapid Identification of Saline-Alkali Stress-Tolerant Peanut Varieties Based on Multimodal Data. *Agronomy* **2025**, *15*, 197. https://doi.org/10.3390/agronomy15010197.
59. Liu, N.; Guo, F.; Li, B.; Jing, Z.; Bai, W.; Hou, X. Comprehensive Evaluation of Ecological Functional Traits and Screening of Key Indicators of Leymus chinensis Germplasm Resources from Northern China and Mongolia. *Agronomy* **2023**, *13*, 1880. https://doi.org/10.3390/agronomy13071880.

60. Li, X.; Luo, L.; Shi, X.; Li, S.; Wang, L.; Li, D.; Li, F. Screening drought tolerance in potato germplasm resources in the northwestern region of China. *BMC Plant Biol.* **2025**, *25*, 777. https://doi.org/10.1186/s12870-025-06716-2.
61. Xue, Y.; Wei, Z.; Zhang, C.; Wang, Y.; Cao, D.; Tang, X.; Yao, Y.; He, W.; Chen, C.; Nisa, Z.u.; et al. Integrated Evaluation of Alkali Tolerance in Soybean: Linking Germplasm Screening with Physiological, Biochemical, and Molecular Responses. *Plants* **2026**, *15*, 222. https://doi.org/10.3390/plants15020222.
62. Li, H.; Xu, C.; Han, L.; Li, C.; Xiao, B.; Wang, H.; Yang, C. Extensive secretion of phenolic acids and fatty acids facilitates rhizosphere pH regulation in halophyte Puccinellia tenuiflora under alkali stress. *Physiol. Plant.* **2022**, *174*, e13678. https://doi.org/10.1111/ppl.13678.
63. Sharma, M.; Saxena, S.; Gaikwad, K.; Batish, D.R.; Siddiqui, M.H.; Alamri, S.; Khan, S.; Al-Munqedhi, B.M.A.; Singh, H.P. Anthocyanin biosynthesis enhances alkali stress tolerance by upregulating antioxidant machinery and modulating ROS levels in three red landraces of rice. *BMC Plant Biol.* **2025**, *25*, 1649. https://doi.org/10.1186/s12870-025-07519-1.
64. Ma, J.; Liu, R.; Zhou, Z.; Zhang, Q.; Shi, G. Integrative transcriptomic and metabolomic analyses reveal crucial roles of phenylpropanoid-derived coumarin biosynthesis in the responses of peanut to iron deficiency. *Environ. Exp. Bot.* **2025**, 238, 106250. https://doi.org/10.1016/j.envexpbot.2025.106250.
65. Han, M.; Tan, Q.; Yang, Y.; Zhang, H.; Wang, X.; Li, X. Integrative Transcriptomic and Metabolomic Insights into Saline-Alkali Stress Tolerance in Foxtail Millet. *Plants* **2025**, *14*, 1602. https://doi.org/10.3390/plants14111602.
66. Lei, L.; Zhou, J.; Ding, G.; Cao, L.; Luo, Y.; Chen, L.; Ren, Y.; Wang, J.; Liu, K.; Lei, Q.; et al. Fine-Mapping and Candidate Gene Analysis of qAT3 for Alkalinity Tolerance in Rice. *Agronomy* **2026**, *16*, 393. https://doi.org/10.3390/agronomy16030393.
67. Peng, X.; Zhou, X.; Sun, Z.; Wu, X.; Teng, C.; Hou, W.; Li, P.; Zheng, D.; Zhang, H.; Fan, H.; et al. Comprehensive evaluation of compound saline-alkali tolerance and gene mining by GWAS in *Vicia faba* L. *BMC Plant Biol.* **2025**, *25*, 1239. https://doi.org/10.1186/s12870-025-07249-4.
68. Jiang, H.; An, H.; Yang, W.; Zhang, X.; Chai, J.; Hao, Y.; Wang, B.; Zhou, G.; Fu, T.; Yang, Z. Screening of Saline-Alkali-Tolerant Rapeseed Varieties Through Multi-Index Integrated Analysis Across the Entire Growth Cycle. *Agronomy* **2025**, *15*, 2046. https://doi.org/10.3390/agronomy15092046.
69. Chai, H.; Wang, X.; Yang, Z.; Li, S.; Xu, Y.; Wu, Y.; Shen, Z. Comparative transcriptome analysis of differentially expressed genes of Medicago falcata L. breeding lines response to saline-alkali stress. *BMC Plant Biol.* **2025**, *25*, 623. https://doi.org/10.1186/s12870-025-06599-3.
70. Fei, L.; Xionghui, B.; Mengjiao, L.; Aijing, H.; Baolong, X. Decoding the saline-alkali tolerance nexus in soybean: A dual-method evaluation model coupled with co-expression networks identifies core regulatory genes. *Front. Plant Sci.* **2025**, *16*, 1699904. https://doi.org/10.3389/fpls.2025.1699904.
71. Nayab, A.; Ayub, A.; Urooj, F.; Ayub, A.; Ahmad, K.; Yipeng, Z.; Ahmed, S.; Sohail, H.; Wu, Y. Molecular and Physiological Insights into CAT- and SOD-Associated Redox Homeostasis Under Salt Stress in Artemisia argyi. *Int. J. Mol. Sci.* **2026**, *27*, 7748. https://doi.org/10.3390/ijms27177748.
72. Miroshnichenko, D.; Klementyeva, A.; Sidorova, T.; Pushin, A.S.; Dolgov, S. Genetic Transformation of Potato without Antibiotic-Assisted Selection. *Horticulturae* **2024**, *10*, 222. https://doi.org/10.3390/horticulturae10030222.
73. Wang, P.; Si, H.; Li, C.; Xu, Z.; Guo, H.; Jin, S.; Cheng, H. Plant genetic transformation: Achievements, current status and future prospects. *Plant Biotechnol. J* **2025**, *23*, 2034–2058. https://doi.org/10.1111/pbi.70028.
74. Ramasamy, M.; Li, G.; Guo, L.; Fang, H.; Eid, A.; Mandlik, R.; Cheng, Y.; Niedz, R.P.; Culver, J.N.; Coleman, G.D.; et al. Boosting genome editing in perennial plants by CRISPR-Combo mediated morphogenic gene activation. *Nat. Commun.* **2026**, *17*, 10201. https://doi.org/10.1038/s41467-026-76367-w.
75. Bai, J.; Jin, K.; Qin, W.; Wang, Y.; Yin, Q. Proteomic Responses to Alkali Stress in Oats and the Alleviatory Effects of Exogenous Spermine Application. *Front. Plant Sci.* **2021**, *12*, 627129. https://doi.org/10.3389/fpls.2021.627129.
76. Rui, C.; Chen, X.; Xu, N.; Wang, J.; Zhang, H.; Li, S.; Huang, H.; Fan, Y.; Zhang, Y.; Lu, X.; et al. Identification and Structure Analysis of KCS Family Genes Suggest Their Reponding to Regulate Fiber Development in Long-Staple Cotton Under Salt-Alkali Stress. *Front. Genet.* **2022**, *13*, 812449. https://doi.org/10.3389/fgene.2022.812449.
77. Liang, Q.; Liu, J.N.; Fang, H.; Dong, Y.; Wang, C.; Bao, Y.; Hou, W.; Zhou, R.; Ma, X.; Gai, S.; et al. Genomic and transcriptomic analyses provide insights into valuable fatty acid biosynthesis and environmental adaptation of yellowhorn. *Front. Plant Sci.* **2022**, *13*, 991197. https://doi.org/10.3389/fpls.2022.991197.
78. Geng, S.; Gao, W.; Sun, F.; Yang, N.; Ma, T.; Wang, T.; Wang, B.; Wang, J.; Qian, S.; Li, S.; et al. Integrated transcriptomic and metabolomic analyses provide new insights into alkali stress tolerance in Gossypium hirsutum. *Front. Plant Sci.* **2025**, *16*, 1604606. https://doi.org/10.3389/fpls.2025.1604606.

79. Yu, Y.; Huang, W.; Chen, H.; Wu, G.; Yuan, H.; Song, X.; Kang, Q.; Zhao, D.; Jiang, W.; Liu, Y. Identification of differentially expressed genes in flax (*Linum usitatissimum* L.) under saline–alkali stress by digital gene expression. *Gene* **2014**, *549*, 113–122. https://doi.org/10.1016/j.gene.2014.07.053.
80. Chen, C.; Dai, J.; Xu, N.; Zhou, W.; Xu, L.; Pang, Q.; Duanmu, H.; Li, H. GsCYP93D1, a Cytochrome P450 Gene from Wild Soybean, Mediates the Regulation of Plant Alkali Tolerance and ABA Sensitivity. *Plants* **2025**, *14*, 2623. https://doi.org/10.3390/plants14172623.

Disclaimer/Publisher's Note: The statements, opinions and data contained in all publications are solely those of the individual author(s) and contributor(s) and not of MDPI and/or the editor(s). MDPI and/or the editor(s) disclaim responsibility for any injury to people or property resulting from any ideas, methods, instructions or products referred to in the content.